The dynamical origin of physiological instructions used in birdsong production

Ezequiel M. Arneodo, Leandro M. Alonso, Jorge A. Alliende, Gabriel B. Mindlin
Departamento de Física FCEyN, Universidad de Buenos Aires

Abstract. In this work we report experimental measurements of pressure patterns used in canary song. We find that these patterns are qualitatively similar to the subharmonic solutions of a simple dynamical system. This is built to account for the activities of subpopulations of neurons arranged in a simple architecture compatible with anatomical observations. The consequences of Hebbian plasticity in the coupling between the driving and the driven systems are outlined.

1. Introduction

Songbirds are an adequate animal model to investigate how complex behavior might be learned. About 40 percent of the known bird species require a tutor for learning. This means that some degree of exposure to an adult song, and posterior practice, are necessary to produce the species specific vocalizations [1]. For this reason, an active field of research has been established which aims at unveiling how the song is produced [2], [3], which physiological instructions drive the avian vocal organ, where in the brain these instructions are generated [4], and ultimately, how the neural network necessary to produce them is reconfigured through experience [5].

Within that research program, physical models for the avian vocal organ (called syrinx) were developed [6], [7], [8]. Those models allowed to explore the relative role played by different biophysical parameters in the determination of the acoustic features generated by the syrinx. Although the delicate coordination of a variety of intrinsic muscles is necessary to produce normal song, many important acoustic features could be reproduced with an adequate air sac pressure gesture and activity of the muscle known as syringealis ventralis [7], which in many oscines is responsible for the control of a syllable's fundamental frequency [9]. Other muscles are known to control the gating of airflow through the syrinx, and prepare it in its phonatory configuration [10], [11].

The precise control of respiratory and vocal muscles requires the coordinated activity of a large number of neurons. In the brain of birds, neurons are organized in cell clusters, known as nuclei [4]. Some of them have been found to play a major role in the generation of the motor gestures necessary for singing [12]. Among these stands the nucleus known

as RA (robustus archistratum), which controls the respiratory gestures during song. Its role is to transform higher level neural activity into precise premotor outputs [13]. Its anatomy has been described [14] and it is known to present a circuitry interconnecting neurons associated with the control of respiration, as well as the activity of the muscles of the vocal organ [15]. Functionally, the neurons in this nucleus are driven by a higher level cell structure known as the high vocal center (HVC) in order to generate a vocalization [16]. This delicate mechanism has been unveiled by measuring the activities of several neurons simultaneously to the uttered song. Yet, given the large number of neurons involved it is hard to associate the registered activity with specific features of the integrated physiological instructions controlling the syrinx.

In this work, we show that pressure patterns used ubiquitously by canaries (*serinus canaria*) during song are similar to the subharmonic solutions of periodically driven low dimensional neural networks compatible with the anatomical observations of the RA nucleus. Under the hypothesis that the diversity of syllable emerges as subharmonic solutions, we explore the consequences of including Hebbian plasticity between the forcing and forced nuclei.

2. Pressure patterns in Canary song

In figure 1(a) we display the time series corresponding to the air sac pressure recorded from a singing bird. It was registered by the insertion of a cannula venisystems Abbocath-T through the abdominal wall just posterior to the last rib, extended a few millimeters into a thoracic air sac. The free end of the cannula was connected to a piezoresistive pressure transducer Fujikura model FPM-02PG, mounted on the bird's back. The signal was amplified and modulated in order to record it using a PC with a sound card MAYA1010. The same card was used to record the ambient sound. A population of four male canaries was analyzed. These four birds were bought from independent breeders, and therefore had different learning experiences. Analyzing the structure of their pressure patterns we found that a number of them were present in every bird. They were observed in an independent population of waterslager canaries [17]. These patterns are displayed in figure 1(b). The first one can be described as an harmonic oscillation, and in our population was present at several syllabic frequencies ranging from 13 ± 2 Hz to 23 ± 2 Hz. The second pattern type presents two maxima per period, and in our population appeared at syllabic rates within the 8 ± 2 Hz and 12 ± 2 Hz. At low syllabic frequencies (between 2 Hz and 5 Hz), a third type of pattern is generically found, which consists of a first peak followed by a slow decay of its pressure value. Finally, a fourth gesture has been found ubiquitously, consisting of fast oscillations mounted on a DC value. These oscillations were produced at a 27 ± 4 Hz-35 ± 5 Hz rate. The syllabic rate region of existence of each gesture type is displayed in figure 2. Notice that this classification of pressure gestures forces to group within the same class song segments presenting different acoustic features. For example, simple harmonic solutions can give rise to vocalizations which are either upsweeps or downsweeps (*i.e.* syllables where the frequency at the beginning of the sound is larger (smaller) than frequency at the end).
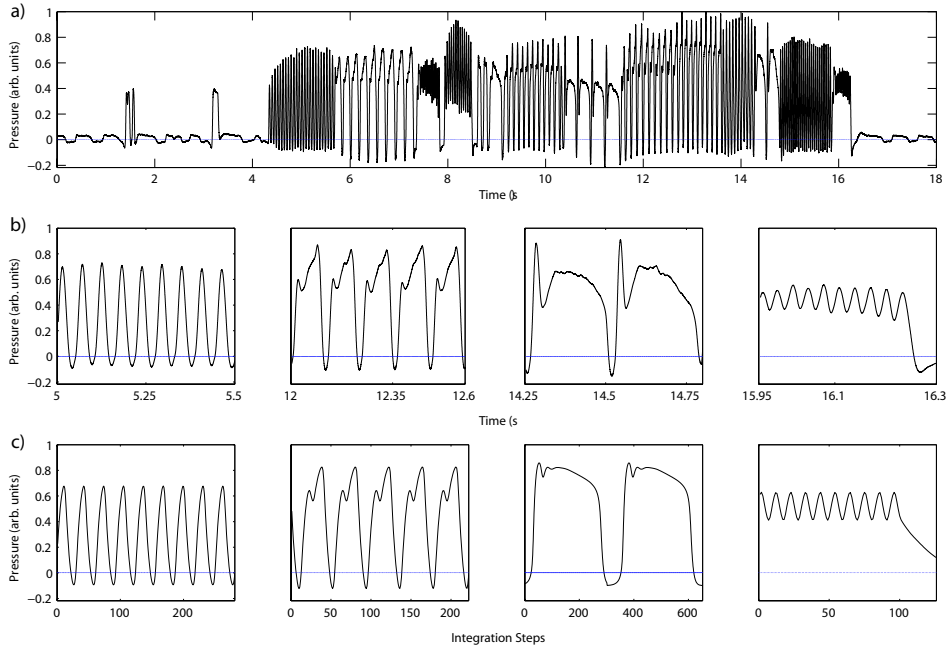
Figure 1. The time trace of the air sac pressure measured during a song. In each presssure pulse, a vocalization takes place. Different patterns are repeated a few times during the time course of the vocalization (a). Ubiquitous pressure patterns used in song production (b). The synthetic pressure patterns generated by the numerical integration of the dynamical system described in the text (see Eqs. (1, 2) where $(a, b, c, d) = (10, 10, 10, -2)$) (c). The values for the forcing parameters (A, w, ρ_x, ρ_y) are, respectively for the four panels from left to right $(2.1, 23, -3.7, -9.5)$, $(2.4, 30, -4, -8.5)$, $(1, 1.5, -6, -8.5)$, $(2, 60, -3.7, -7.5)$.
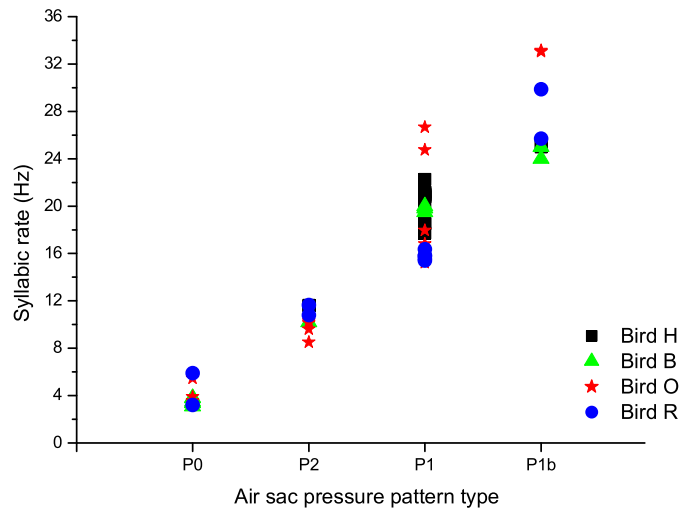
Figure 2. The syllabic rates at which different syllable types are generated by the birds analyzed in our experiment. The different point types denote different analyzed birds. Each point represents a syllable; the horizontal axis stands for the air sac pressure type, and the vertical axis indicates the syllabic rate. Notice the clustering of different patterns along the verical axis in well defined ranges. A pattern of the type which we call P1 is displayed in the first panel (from left to right) in figure 1(b). Patterns called P2, P0 and P1b in this figure are shown in the second, third and fourth panels of figure 1(b) respectively.

3. Model for the generation of pressure patterns

The brain structure controlling song production in songbirds consists of sets of neurons called nuclei and axons interconnecting them, forming a circuit known as the motor pathway. Its output is the nucleus RA, which consists of at least two classes of projections neurons. In the most dorsal region of RA one finds neurons projecting to the respiratory premotor nuclei. The neurons that project into the premotor neurons innervating syringeal muscles are located in the ventral region of RA. These neurons are interconnected by long inhibitory ones, which have been conjectured to link disparate regions of RA, coordinating the firing of multiple RA projection neurons [14]. During singing, RA neurons generate sequences of action potential bursts, typically a few bursts of about 10 ms, well time locked with part syllables [18]. Work on zebra finches (*Taeniopygia guttata*) has shown that during the singing of a motif (a sequence of a diversity of syllables), each RA-projecting HVC neuron is active only during a brief amount of time (about 6ms). In this way, RA neurons are driven by different RA-projecting HVC neurons, each being active during a small time window. The high interconnectivity of the RA circuitry precludes this detailed picture from predicting the total output of the nucleus. On the other hand, the lack of a qualitative theory of extended nonlinear systems interposes between computational implementations of this mechanism [19] and the calculation of global nuclei activity. In this work we explore the hypothesis that the average activity on parts of the nuclei can account for the oberved patterns. We also explore the hypothesis that the distinctive features described above are generated at the level of the RA nucleus, and that those instructions are followed by the respiratory nuclei during song production. In this way, we will build a model in which the repetitive syllables in canary song are initiated with periodic fluctuations of the average activity in the HVC nucleus, which drives the activity of RA. Due to the existence of excitatory and inhibitory subpopulations in RA, driving activity of different frequencies can generate subharmonic solutions. We will then explore the hypothesis that the distinctive features experimentally recorded can be interpreted in terms of the subharmonic solutions of RA subpopulations under periodic forcing. The dorsal part of the nucleus RA contains both inhibitory interneurons and excitatory neurons; these last projecting to the respiratory nuclei [15] (see figure 3(a)). We will describe a computational model for the activity of these populations in terms of two variables x and y, whose dynamics will be ruled by an additive model [20]:

$$\tau \frac{dx}{dt} = 15(-x + S(\rho_x + ax - by + A\cos(wt))) \tag{1}$$

$$\tau \frac{dy}{dt} = 15(-y + S(\rho_y + cx - dy)), \tag{2}$$

where $\rho_x + A\cos(wt)$ and ρ_y stand for the input activity after substraction of a threshold value, the sigmoideal function $S(x) = 1/(1 + exp(-x))$ mimics the saturating nature of the response of the nuclei activity, and the signs in the coefficients of x and y are compatible with the excitatory (inhibitory) nature of x (y). The values of (a, b, c, d) are listed in the caption of figure 1. The different solutions that this system can display without the temporal part of the input forcing (*i.e.* $A = 0$) have been described in [20], and a schematic summary is displayed in figure 3(b). Since among them we find wide regions of the parameter space that are excitable, and others where the dynamics is oscillatory, it is to be expected that under the action of periodic driving, the system will display subharmonic

solutions [21]. In figure 1(c), we show the different solutions of the driven model for the excitatory and inhibitory supopulations of RA, for different values of the input forcing (see values in the figure caption). The different solutions can be characterized by their periodicity measured in units of the forcing period. The solution displayed in the first panel of figure 1(c) is a period 1 solution (*i.e.* it repeats itself after a time equal to the forcing period). The solution displayed in the second panel, on the other hand, is a period 2 solution. In this way, a lower sylabic rate is achieved through an increase of the driving force. Beyond this topological characterization, some morphological features can be added to our description.

For example, the solutions displayed in the third and fourth panels of figure 1(c) are also period one solutions, yet, they are morphologically very different. The generation of the solution shown in the third panel required a very slow driving. Since the driving is slow (compared to the characteristic times of the non forced system), we can interpret the shape of the solution with the help of the bifurcation diagram without the forcing. The solution starts at a fixed point where the variable x is not activated. As the driving is increased, the system develops an attractive focus, and therefore the trajectory presents a few wiggles that are a signature of its transient decay to this activated state. As the driving input ρ_x is decreased, this fixed point is anhilated, and the system returns to its inactive fixed point. The arrows in figure 3(b) describe this parameter excursion. Finally, the last solution is achieved for high forcing frequencies. This new period one is qualitatively different to the one displayed in the first panel: it sweeps a small region of the parameter space, and it is dynamically born in a period halving of the solution shown in the second panel. Notice that the three solutions were obtained when the same neural architecture was subjected to different forcings. The location of the panels with respect to those in the bottom panels of figure 1(b) was chosen to highlight the qualitative similarities with the recorded pressure in singing canaries. The solutions described above exist in wide regions of the parameter space, and no algorithmic procedure was used to adjust them to the values reported in the figure caption. The solutions chosen to illustrate the responses of the system are representative of those found in wide tongues of the parameter space. In the framework of the experimental data, we interpret these tongues as the finite width of the syllabic ranges where the different pressure patterns are found for all the birds in our study (see figure 2).

4. The dynamics of Hebbian learning

The process by which learning takes place in songbirds is not yet understood. It is known that another set of nuclei, constituting what is known as the anterior forebrain pathway (AFP) is necessary [4], [22], but the nature of the instructions that the output of this pathway (the nucleus known as LMAN) sends to the motor pathway (more prcisely, to RA), has not been unveiled. Yet, under the hypothesis that the pressure patterns emerge as subharmonic responses of parts of the the nucleus RA under a periodic forcing by nucleus HVC, the connection between these two should evolve in time, due to Hebbian learning. Therefore, it is natural to ask how Hebbian learning affects the existence of subharmonic responses of a nonlinear forced system. In particular, we are interested in investigating in which ranges of forcing frequency it is possible to find sub harmonic lockings, once the temporal evolution of the coupling between forced and forcing systems is taken into ac-
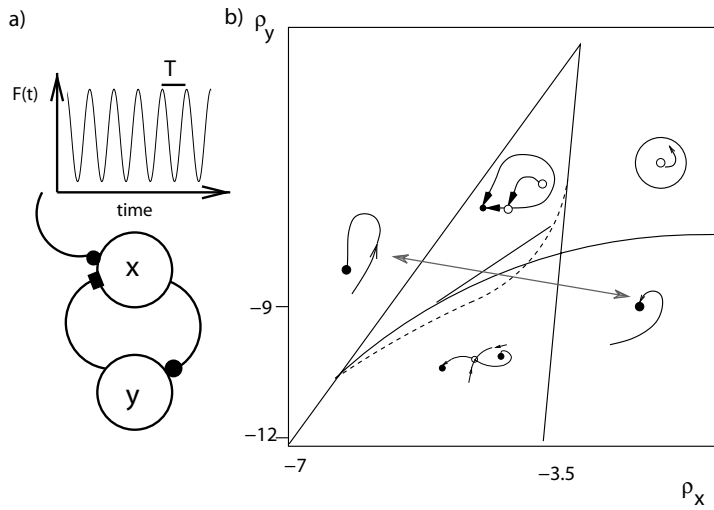
Figure 3. A schematic drawing of the neural subpopulations whose activities we model with equations (1), (2) (a). The parameter space of the homogeneous model (without forcing). For different parameter values (ρ_x, ρ_y), qualitatively different solutions exist, separated by bifurcation lines. The arrows indicate a path used to generate a low rate pressure pattern (see text) (b).

count. The four patterns in figure 1(b) are present in every bird that we studied. Moreover, the syllables of the first and second pannel appear in almost every analyzed song. For this reason, at this poit we will focus in how plasticity affects the lockings $1:1$ and $1:2$.

In terms of equations (1,2), one is interested in including a dynamical rule for the coupling parameter A, which should satisfy the Hebbian hypothesis, namely: 1. Learning involves the modification of synaptic connections between populations, 2. Learning is local 3. The modifications are slow and 4. If either population is silent, the modification of synaptic strength is an exponential decay [20]. Writing normal forms for Equations (1,2) at the onset of Hopf bifurcations, and reducing their dynamics to the phase equations [23], we write close to the resonant cases $1:1$, $1:2$ the bidimensional dynamical systems that account for the dynamics of A and $\phi_2 - \phi_1$, $2\phi_2 - \phi_1$ respectively, where ϕ_2 and ϕ_1 describe the phases of the driven system and its driver (see caption of figure 4, where the equations and parameters are listed). Notice that in order to account for a long term effect of Hebbian plasticity when resonances are investigated, we have to include high order terms in the equation describing the dynamics of A. In this way, we can compute the ranges of frequencies for which locking is possible, for the resonant cases explored in this work as illustration. Figure 4 shows the results, which can be described qualitatively as a sharpening of the locking regions compared to those of the forced system with a static coupling.
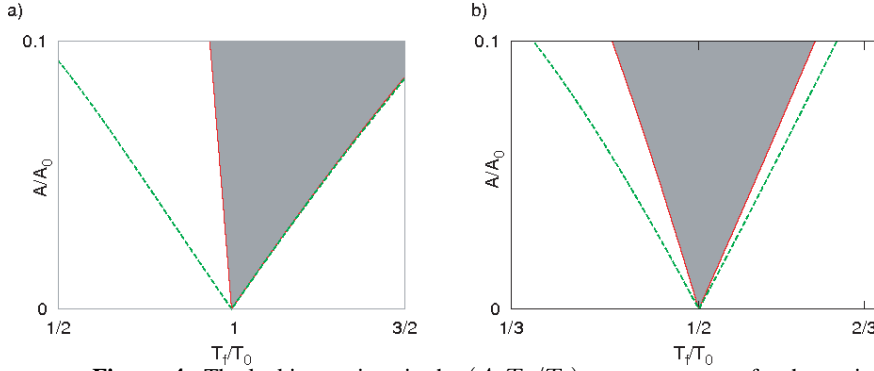

Figure 4. The locking regions in the $(A, T_f/T_0)$ parameter space for the static coupling case (dashed lines) and plastic coupling (shadowed region within continuous lines) for two resonances: $1:1$ (a) and $1:2$ (b). $T_f = 2\pi/\omega_f$ and $T_0 = 2\pi/\Omega_0$ are, respectively, the periods of the driver and the driven system. The equations ruling the dynamics of the phases and coupling parameters close to each of the resonances are: $\dot{\chi}_1 = \Omega_0 - \omega_f - A B_3 \cos(\chi_1 - \delta_3)$; $\dot{A} = -A + \Gamma A r_2 \cos(\chi_1)$ for the 1:1 case, $\dot{\chi}_2 = 2\Omega_0 - \omega_f - 2 A B_0 \sqrt{1 + \left(\frac{\beta_1}{\alpha_1}\right)^2} \cos(\chi_2 - \delta_0 - \delta_1)$; $\dot{A} = -A + \Gamma A r_2^2 \cos(\chi_2)$ for the 1:2 case. We have defined variables $\chi_1 = \phi_2 - \phi_1$, $\chi_2 = 2\phi_2 - \phi_1$. All the other parameters $(\alpha_1, \beta_1, \delta_1, B_3, \delta_3, B_4, \delta_4, \Omega_0, r_2) = (-17.92, 25.31, 5.67, 68.45, 0.23, 42.68, 2.57, 3.23, 0.24)$ arise from transforming Eqs. (1,2) for (a, b, c, d) as listed in the caption of figure 1 into the dynamical equations written above on the onset of the Hopf bifurcation, where $(\rho_y = -8.85, \rho_x = -0.40)$. The values for (B_0, δ_0) depend on ω_f (see appendix). The borders of the tongues found in the model with plasticity are determined by the saddle node bifurcations at which fixed points for the equations above are born.

5. Discussion and conclusions

In this work we analyzed simultaneous records of sound and air sac pressure patterns during canary song production. Four male canaries were used in our study. Despite the diversity of acoustic features present in the songs, we found that some pressure patterns, produced at different syllabic rates, can be found in all the birds. Remarkably, the birds came from different breeders, and therefore were not subjected to the same tutoring. The different pressure patterns were generated, by each bird, at different syllabic rates. Pressure patterns presenting similar morphological features were produced at rates which cluster in different ranges.

In our work, we show that the different morphological features can be explained as those presented by the sub harmonic responses of simple nonlinear neural architectures, providing us with a simple way to generate a wide diversity of behavioral responses. The choice of (a, b, c, d) in Eqs. (1,2) guarantees the existence of both excitable and oscillatory dynamics for the autonomous system in the region of parameters explored. These dynamical conditions ultimately allow us to find subharmonic responses under periodic forcing.

Although the biological processes involved in birdsong learning are yet to be understood, we started investigating the effect of Hebbian plasticity in a forced nonlinear system which presents subharmonic behavior. We show that when the dynamics of the coupling parameter is taken into account, the ranges of frequencies where locking is possible get reduced.

6. Appendix

The values of parameters (B_0, δ_0), are given by

$$
\begin{aligned}
B_0 &= \sqrt{\alpha_0^2 + \beta_0^2} \\
\tan \delta_0 &= \frac{\beta_0}{\alpha_0},
\end{aligned}
\tag{3}
$$

where (α_0, β_0) are the real and imaginary part of the coefficient of the only cuadratic resonant term in the normal form of the system (1,2) close to the $2:1$ resonance.
In the same way, we obtain the values of parameters $(\delta_1, \delta_3, B_3)$:

$$
\begin{aligned}
\tan \delta_1 &= \frac{\alpha_1}{\beta_1} \\[1em]
\tan \delta_3 &= \frac{\beta_1 (\beta_2 - \beta_3) - \alpha_1 (\alpha_3 - \alpha_2)}{\beta_1 (\beta_2 + \beta_3) - \alpha_1 (\alpha_2 + \alpha_3)} \\[1em]
B_3 &= \frac{\sqrt{[\beta_1 (\alpha_3 + \alpha_2) - \alpha_1 (\beta_3 + \beta_2)]^2 + [\alpha_1 (\alpha_3 - \alpha_2) + \beta_1 (\beta_3 - \beta_2)]^2}}{\alpha_1^{3/2}},
\end{aligned}
\tag{4}
$$

where (α_i, β_i) are respectively the real and imaginary parts of the coefficients of each of the three cubic resonant terms of the normal form reduction of the system defined by equations (1,1) when $\omega_f \approx \Omega$.

References

[1] P. Marler and H. Slabbekoorn, *Nature's Music, the science of birdsong* Elsevier, San Diego, (2004).

[2] F. Goller and R.A. Suthers, Nature **373** 63-66 (1995).

[3] R.A. Suthers, "How birds sing and why it matters", in *Nature's Music, the science of birdsong* Elsevier, San Diego,P. Marler and H. Slabbekoorn, Editors, 272-295 (2004).

[4] E. D. Jarvis, "Brains and Birdsong", in *Nature's Music, the science of birdsong* Elsevier, San Diego,P. Marler and H. Slabbekoorn, Editors, 226-271 (2004).

[5] A J. Doupe, M. M. Solis, R. Kimpo and C. A. Boetinger, Ann. N.Y. Acad. Sci. 1016: 495-523 (2004).

[6] Gardner T., Cecchi G., Magnasco M., Laje R., Mindlin, G.B Phys. Rev. Letts. **87** art. 2008101 1-4 (2001).

[7] Laje R. and Mindlin G. B. (2002). Neuromuscular control of vocalizations in birdsong: a model. *Phys. Rev. E* **65** art. 051921, 1-8.

[8] Mindlin G.B., Gardner T. J., Goller F. and Suthers R. (2003) Phys. Rev. E **68** art. 04198.

[9] F. Goller and R.A. Suthers (1996), J. Neurophysiol. **75** 867-876.

[10] Suthers R. A., Goller F. and Pytte C. The neuromuscular control of birdsong. Phil. Trans. R. Lond. B 354, 927-939 (1999).

[11] G. B. Mindlin and R. Laje *The physics of birdsong* Springer, New York (2005).

[12] F. Nottebohm and A. P. Arnold (1976) Science **194** 211-213.

[13] A. C. Yu and D. Margoliash (1996), Science **273** 1871-1875.

[14] Sturdy C. B. Wild J. M. and Mooney R. Respiratory and telencephalic modulation of vocal motor neurons in the zebra finch. J. Neurosci. 23, 1072-1086 (2003).

[15] Spiro J, Dalva M, Mooney R (1999), J Neurophysiol **81**: 3007-3020.

[16] R. H. Hahnloser, A. A. Kozhevnikov and M. S. Fee (2002) Nature **419** 65-70.

[17] M. A. Trevisan, G. B. Mindlin and F. Goller, Phys. Rev. Letts., **96** 058103 (2006).

[18] Z. Chi and D. Margoliash (2001), Neuron **32** 899-910.

[19] H. D. I. Abarbanel, L. Gibb, G. B. Mindlin and S. Talathi (2004), J. Neurophysiol. **92** 96-110.

[20] Hoppensteadt F. C., Izhikevich E. M., Weakly connected neural networks, Springer-Verlag New York, Inc., Secaucus, NJ, (1997).

[21] Piro O. and Gonzalez D., Phys. Rev. A 37, 4060-4063 (1988).

[22] M. S. Brainard and A. J. Doupe, Nature **417** 351-358 (2002).

[23] Pikovsky, A., Ronsenblum, M., and Khurths, J., Synchronization, Cambridge University Press (2001).